

Combining bioaccumulation and coping mechanism to enhance long-term site-specific risk assessment for zinc susceptibility of bivalves

Bo-Ching Chen^a, Wei-Yu Chen^b, Yun-Ru Ju^b, Jeng-Wei Tsai^c, Li-John Jou^d, Sher Singh^e, Chung-Min Liao^{b*}

^a *Department of Post-Modern Agriculture, MingDao University, Changhua, Taiwan 52345, ROC*

^b *Department of Bioenvironmental Systems Engineering, National Taiwan University, Taipei, Taiwan 10617, ROC*

^c *Institute of Ecology and Evolutionary Biology, China Medical University, Taichung, Taiwan 40402, ROC*

^d *Department of Biomechatronic Engineering, National Ilan University, Ilan, Taiwan 26047, ROC*

^e *Department of Life Science, National Taiwan Normal University, Taipei, Taiwan 11677, ROC*

*Corresponding author. Tel: +886-2-2363-4512; Fax: +886-2-2362-6433; e-mail: cmliao@ntu.edu.tw

Abstract

1. Introduction

Zinc (Zn) is an essential micronutrient for almost all aquatic organisms. This transition metal is responsible for many biochemical processes including regulatory, structural, and enzymatic functions (Tsai et al., 2006). Within its optimal range of concentration, Zn plays a critical role in growth, physiology, and development for aquatic organisms (Sappal et al., 2009). If waterborne Zn levels are elevated, however, toxicity can occur and have severe effects on the health of aquatic organisms. The primary toxic actions of Zn are its disturbance of normal enzymatic activities, depletion of glutathione, and substitution for essential metals such as calcium (Tsai et al., 2006). Typical concentrations of Zn in unpolluted waters range from 0.02 to 5 $\mu\text{g L}^{-1}$ (Luoma and Rainbow, 2008). Due to intensive human activities (e.g., mining, disposal of batteries, and use of fertilizers), however, Zn has been found at high levels in some aquatic ecosystems. For instance, previous investigations indicated that Zn was detected in many rivers and that maximum Zn concentrations in contaminated aquacultural waters were reported to range from 60 to 130 $\mu\text{g L}^{-1}$ in different areas in Taiwan (Lee et al., 1996). Consequently, Zn contamination in aquatic ecosystems has been received increasing attention worldwide in recent years.

For the water quality management purpose, it is important to be able to continuously, real-time monitor contaminant levels in aquatic ecosystems. Bivalves such as clams and mussels are considered ideal candidates for biomonitoring contaminants in aquatic ecosystems due to their wide distribution, extensive population, sedentary nature, and the ability to accumulate contaminants (Liao et al., 2005). Recently, there have been extensive studies focused on the establishment of biological early warning systems by continuously tracking the physiological or behavioral changes of bivalves in response to the occurrence of metals in the aquatic

environment (Liao et al., 2008; 2009). However, little is known on the mechanisms of metal uptake by bivalves and the subsequent effect associated with metal exposure.

The process of accumulation of waterborne metals by aquatic organisms is defined as bioaccumulation. The bioconcentration factor (BCF), which relates the concentration of metals in water to their concentration in aquatic organisms at equilibrium, is generally used to estimate the propensity to accumulate metals in the organism (Liao et al., 2003). Over the past decade, the BCF has been extensively studied by the biokinetic model that incorporates aqueous uptake and efflux. These biokinetic parameters, including uptake and elimination rate constants, are known to be affected by several environmental and physiological factors such as dissolved metal concentration, salinity, and the body size and sex of the organisms (Chong and Wang, 2001; Shi and Wang, 2004; Wang and Rainbow, 2006). The whole body burden obtained from the biokinetic model was then used to construct the dose-response relationship and to predict the toxic effect based on the toxicokinetic/toxicodynamic model.

Recently, numerous studies highlight the importance of applying the subcellular partitioning of metals within the organism, instead of whole body burden, to link metal bioaccumulation to the potential biological effects (Wang and Rainbow, 2006; Martin et al., 2007; Kamunde, 2009). Within this concept, it is generally suggested that the accumulated metal can approximately be divided into two subcellular pools: (i) metabolically active pool (MAP, including organelles, microsomes, and heat-labile proteins), and (ii) metabolically detoxified pool (MDP, including metallothionein-like proteins and metal-rich granules). The metal accumulated in MDP is presumed to be of no toxicological effect, whereas adverse physiological consequence was associated with the metal levels in MAP. Therefore, coupling of the biokinetic model and the

subcellular partitioning model can enhance our ability to better characterize the mechanism of metal bioaccumulation as well as to predict toxicological effects of the metal on aquatic organisms.

Despite the importance of subcellular concept, studies on the relationship between intracellular metal concentration and toxicological consequence are still limited. The damage assessment model (DAM), derived by consideration of the bioconcentration process, damage accumulation process, and damage recovery process, has been used to describe the mode of toxic action of contaminants binding to the target site (Lee et al., 2002; Ashauer et al., 2007). In the DAM, hazard is assumed to accumulate in proportion to the cumulative damage level associated with body residue at the site of action for aquatic organisms. Therefore, the DAM provides a more comprehensive framework which may be applied to predict hazardous effect based on the subcellular metal compartmentalization in aquatic organisms.

From the perspective of ecotoxicology, a combination of the bioaccumulation and coping mechanism can enhance our ability to better predict the susceptibility of aquatic organisms for real field exposure. In practice, given that both physiological parameters of aquatic organisms and geochemistry parameters of ambient water are considered, an integration among bioaccumulation, subcellular partitioning, and hazard accumulation is of potential utility to develop and refine ambient water quality criteria (AWQC). Therefore, it is necessary to link the subcellular concept with the biologically-based DAM to quantify the interactions among metal stressors, receptors, and metal regulation of organisms under a broad range of metal stress-driven environment.

The purpose of this study is to conduct long-term site-specific risk assessment for Zn susceptibility of bivalves based on published experimental data by linking the

biologically-based DAM with the subcellular concept. Two species of saltwater bivalves, the green mussel *Perna viridis* and the hard clam *Ruditapes philippinarum*, are chosen as model organisms because of their high production and economic importance in Taiwan aquaculture industry. Furthermore, these two species can be employed to biomonitor the water quality on Taiwan coastal areas because of their wide distribution in these regions.

2. Materials and methods

2.1 Model development

There are three consecutive steps involved in modeling susceptibility probability of bivalves exposed to waterborne Zn: (i) the internalization of waterborne Zn to bivalves, (ii) the subcellular distribution of Zn within bivalves, and (iii) the hazardous effects caused by Zn accumulated in MAP. In the present study, a first-order one-compartment bioaccumulation model was employed to estimate whole body burden of bivalves exposed to waterborne Zn. The Zn accumulated was then divided into two subcellular pools: MAP and MDP. Finally, proportion of accumulated Zn in the potentially sensitive subcellular compartment (i.e., MAP) was adopted to represent physiological response of bivalves by DAM. In addition, steady-state conditions were considered throughout the model derivation to reflect the long-term exposures experienced in the field circumstance. The overall methodology used to predict the susceptibility of bivalves exposed to waterborne Zn and the subsequent site-specific risk assessment was depicted in Fig. 1.

2.1.1 Bioaccumulation model

In the present study, the rate of change of Zn concentration in bivalves, $C_b(t)$ ($\mu\text{g g}^{-1}$), was assumed to follow a first-order one-compartment model

$$\frac{dC_b(t)}{dt} = k_u \cdot C_w - k_e \cdot C_b(t), \quad (1)$$

where C_w is the dissolved Zn concentration in water ($\mu\text{g mL}^{-1}$), t is the exposure duration (d), k_u is the uptake rate constant of Zn in bivalves ($\text{mL g}^{-1} \text{d}^{-1}$), and k_e is the elimination rate constant (d^{-1}). The steady-state bioconcentration factor of bivalves, BCF, can be calculated by definition as

$$\text{BCF} = C_b(\infty) / C_w = k_u / k_e, \quad (2)$$

where $C_b(\infty)$ is the steady-state Zn concentration in bivalves. Therefore, BCF can be viewed as a multiplier which can relate external concentration in environmental medium to internal concentration in organisms.

2.1.2 Zinc compartmentalization within bivalve

The steady-state Zn concentration in bivalves estimated from Eq.(2) was divided into two subcellular pools: MAP and MDP. According to the concept proposed by Croteau and Luoma (2009), toxic effects result from the excess of metal influx over the combined rates of elimination and detoxification. The critical value at which metal influx begins to exceed the combined rates is referred to as metal influx threshold (MIT). From the perspective of MIT, the detoxification rate can be estimated as

$$k_d = \frac{k_u \cdot C_w}{C_{MAP, c}} - k_e, \quad (3)$$

where k_d is the detoxification rate constant (d^{-1}), $C_{MAP, c}$ is the metal concentration in metabolically active pool (MAP) without Zn exposure ($\mu\text{g g}^{-1}$). It is suggested that the detoxification and elimination rate constants characterize the proportion of metal accumulated in the MAP relative to MDP, which depends on whether the metal plays an essential role in metabolism (Croteau and Luoma, 2009).

2.1.3 Modeling susceptibility probability

To model the susceptibility probability of bivalves exposed to waterborne Zn, the DAM proposed by Lee et al. (2002) was firstly employed to calculate the steady-state cumulative damage ($D(\infty)$) as

$$D(\infty) = (k_a \cdot BCF \cdot C_w \cdot k_r^{-1}), \quad (4)$$

where k_a is the damage accumulation rate constant ($\text{g } \mu\text{g}^{-1} \text{ d}^{-1}$), k_r is the damage recovery rate constant (d^{-1}). In the DAM concept, the damage recovery rate constant is crucial for characterizing all processes leading to recovery such as repair mechanisms on a cellular scale or adaption of the physiology and other compensating processes (Ashauer et al., 2007).

Secondly, a killing rate constant, k_k ($\text{g } \mu\text{g}^{-1} \text{ d}^{-1}$), was introduced to relate the internal damage accumulation to the steady-state cumulative hazard ($H(\infty)$) as

$$H(\infty) = (k_k / k_a) \cdot D(\infty). \quad (5)$$

It is suggested that the killing rate constant can reflect the toxic potency of the metal on the organisms and can be calculated as $D_{E,50} / k_a$, where $D_{E,50}$ is the cumulative damage for 50% effect (-) (Lee et al., 2002; Ashauer et al., 2007). Therefore, the steady-state, concentration-dependent susceptibility $S(C_w)$ can be derived directly from an exponential relationship of cumulative hazard as (Lee et al., 2002; Ashauer et al., 2007)

$$S(C_w) = 1 - \exp(-H(\infty)) = 1 - \exp(-k_k \cdot BCF \cdot C_w \cdot k_r^{-1}). \quad (6)$$

Lastly, the site-specific susceptibility probability of bivalves exposed to waterborne Zn can be calculated by a joint probability function as

$$P(S(C_w)) = P(C_w) \times P(S(C_w) | C_w). \quad (7)$$

where $P(S(C_w))$ represents the probability risk estimate of waterborne Zn exposure-associated susceptibility, $P(C_w)$ stands for the probability density function of waterborne Zn concentration, and $P(S(C_w)|C_w)$ is the conditional probability.

2.2 Model parameterization

2.2.1 Biokinetic and geochemical parameters

In the present study, uptake rate constants of *P. viridis* and *R. philippinarum* exposed to waterborne Zn were adapted from the experimental data published by Chong and Wang (2001). To account for the uncertainty/variability of BCF in the field, the uptake and elimination rate constants proposed by several previous works (i.e., Chong and Wang, 2001; Blackmore and Wang, 2002; Shi and Wang, 2004) were pooled together to determine the probability distribution of BCF. Elimination rate constants of the bivalves can then be estimated by Eq. (2). Three coastal zones with known water chemistry characteristics at Toucheng, Kouhu, and Pingtung, which located respectively in the north, central, and south areas of Taiwan, were selected to implement the proposed model.

2.2.2 Subcellular fractionation and toxicodynamic parameters

To determine Zn subcellular fractionation, data from the subcellular Zn partitioning proposed by Blackmore and Wang (2002) and Ng and Wang (2004) were summed into MAP (organelles and heat-sensitive proteins) and MDP (metal-rich granules, and metallothionein-like proteins). Proportion of accumulated Zn in the MAP was then employed in Eq. (3) to calculate the detoxification rate constant. The damage recovery rate constant was obtained by fitting the exponential term in Eq. (6)

to the Zn proportions in metallothionein-like proteins of *P. viridis* and *R. philippinarum* under various exposure concentrations. Subsequently, the killing rate constant can also be estimated by known values of the damage accumulation rate, k_a , and the cumulative damage for 50% effect, $D_{E,50}$, obtained from the above-mentioned fitting results.

2.3 Data analysis and model simulation

TableCurve 2D (Version 5.0, AISN Software Inc., Mapleton, OR, USA) was used to fit the published data to obtain the optimal statistical models. The level of significance was set at $p < 0.05$. A Monte Carlo simulation was performed to obtain 2.5th- and 97.5th- percentiles as the 95% confidence interval (CI) for all fitted models. Crystal Ball[®] software (Version 2000.2, Decisioneering, Inc., Denver, Colorado, USA) was employed to implement the Monte Carlo simulation.

Model simulations were carried out by introducing the bioaccumulation parameters, the killing rate constant, the damage recovery rate constant, and the field data of waterborne Zn concentration into Eq. (6) and (7) to assess the site-specific risk for Zn susceptibility of bivalves *P. viridis* and *R. philippinarum*.

3. Results

3.1 Toxicokinetics and subcellular compartmentalization

The biokinetic parameters as well as the subcellular fractionation of *P. viridis* and *R. philippinarum* exposed to waterborne Zn were summarized in Table 1. The best-fitted probability distribution of BCF for *P. viridis* and *R. philippinarum* was determined to be LN (12820 mL g⁻¹, 1.79) and LN (12210 mL g⁻¹, 1.59), respectively (Fig. 2A, B). Very high BCF values with order of magnitude 10⁴ have found for both

species, indicating that a process of bioaccumulation of Zn occurred in the water-bivalve system. The Zn concentration in MAP for *P. viridis* ($71.33 \mu\text{g g}^{-1}$) was double than that for *R. philippinarum* ($36 \mu\text{g g}^{-1}$), suggesting that *P. viridis* accumulates more Zn toxicity. The killing rate constant, k_k , and the damage recovery rate constant, k_r , could then be estimated to be $0.025 \text{ g mg}^{-1} \text{ d}^{-1}$ and 0.19 d^{-1} for *P. viridis* ($r^2 = 0.91$), and $0.13 \text{ g mg}^{-1} \text{ d}^{-1}$ and 0.40 d^{-1} for *R. philippinarum* ($r^2 = 0.98$), respectively (Table 1). These results indicated that both toxic potency and the speed of recovery of Zn are higher for *R. philippinarum* than *P. viridis* (Fig. 2C, D).

3.2 Linkages between bioaccumulation and coping mechanism

The probability distribution of elimination rate constant, obtained from dividing the uptake rate constant by BCF distribution, was LN (0.04 d^{-1} , 1.79) and LN (0.02 d^{-1} , 1.41) for *P. viridis* and *R. philippinarum*, respectively (Fig. 3A, D). The elimination rate constant with known probability distribution was then introduced into Eq. (3) to demonstrate the detoxification rate constant of Zn for bivalves. The resulting distribution of detoxification rate constant was LN (0.93 d^{-1} , 1.77) for *P. viridis* and LN (0.67 d^{-1} , 1.79) for *R. philippinarum*, respectively (Fig. 3B, E).

To represent the relationship between elimination and detoxification mechanism, the joint distributions showing the quantitative linkages between k_e and k_d for *P. viridis* and *R. philippinarum* exposed to waterborne Zn ranged from 0 to $250 \mu\text{g L}^{-1}$ were given in Figure 3C, F. The results revealed (i) negative linear correlations between k_e and k_d for both species under constant exposure concentration; (ii) detoxification rate constant is larger for *P. viridis* than *R. philippinarum* at a given elimination rate constant; and (iii) both k_e and k_d increase with increasing waterborne Zn concentration.

To further explore the substantial interaction among bioaccumulation, detoxification, and subcellular distribution, the correlation between three key parameters in bioaccumulation and coping mechanism (i.e., k_e , k_r , k_d) were also determined under a fixed exposure concentration ($50 \mu\text{g L}^{-1}$), as depicted in Fig. 4. These results showed that negative linear correlations exist for k_e-k_r and k_e-k_d relationship, whereas a positive linear correlation was observed for k_r-k_d relationship for bivalves exposed to waterborne Zn. Therefore, an increase in the Zn proportion accumulated in the MDP accompanied a higher speed of recovery for bivalves. In addition, the two key parameters in coping mechanism can be determined from the experiment-derived bioaccumulation parameter by the k_e-k_r and k_e-k_d relationships as depicted in Fig. 4.

3.3 Site-specific susceptibility probability

The probability distribution of waterborne Zn concentration at Toucheng, Kouhu, and Pingtung was shown in Fig. 5A, C, and E, respectively. The simulation results of the site-specific susceptibility probability of *P. viridis* and *R. philippinarum* exposed to waterborne Zn were presented in Fig. 5B, D, and F. The probability that 50% or more of susceptibility of *P. viridis* population affected by waterborne Zn (risk = 0.5) was 0.19, 0.07, and 0.004 for Toucheng, Kouhu, and Pingtung, respectively. For *R. philippinarum*, the 50% exceedence risk of susceptibility was 0.39, 0.19, and 0.01 for Toucheng, Kouhu, and Pingtung, respectively. These results showed that, for both *P. viridis* and *R. philippinarum*, the susceptibility of Zn to bivalves in selected coastal areas was highest at Toucheng, followed by Kouhu and Pingtung. This may be primary resulted from the spatial variation of waterborne Zn concentration among the three studied sites. Furthermore, the results also indicated that *R. philippinarum* is

more susceptible of Zn than *P. viridis* under the same exposure condition. The results may be due to *R. philippinarum* have slower elimination rate and higher killing rate compared to those for *P. viridis* (Table 1).

4. Discussion

4.1 Metal influx threshold and detoxification

The total accumulated metals in target sites are not necessary for accounting the induced toxicity. The portion that binding to metabolically active pool (metal-sensitive compartment) might be the source for the toxicity. With the analyze of the subcellular distribution of the accumulated metal, we could characterize the biokinetic strategy for regulating or metabolizing the accumulated metal of the contaminated organisms. In the present study, we adopted the metal influx threshold (MIT) approach (Croteau and Luoma, 2009) by linking with subcellular partitioning concept to quantify the detoxification rate (k_d) constant under different exposure scenarios. Our results reveal that the value of k_d increases with increasing exposure concentration (C_w) and shows negative correlation with elimination rate (k_2) (Fig. ?).

Methodology of the MIT assumes that a dose threshold, once the accumulated metal level exceeded the threshold level, the metal influx begins to exceed the combined rates of depuration and detoxification (Croteau and Luoma, 2009). We found that the metal detoxified pool (MDP) is the major fraction accounting the accumulated metal when organism exposed to very low metal concentration. Therefore, we assumed that the metal concentration in fraction of MAP of the control group as the threshold active concentration (有何依據?文獻). The second assumption of MIT is that MAP is the first fraction to accumulate with metals during exposure (Wang and Rainbow, 2006). Consequently, k_d can be estimated with the transportation

rate of the metal from MAP to MDP. Finally, MIT was developed from dietborne metal exposure in the beginning. In this study, we assume that MIT is valid for dietborne and waterborne metal exposure.

The proposed methodology by linking the concept of subcellular partition of the accumulated metal with the MIT approach is useful to quantify the detoxification ability of exposed organisms and provides an opportunity for a more mechanistic-based framework to assess metal-specific and species-specific toxicity.

4.2 Site- and species-specific susceptibility

The physiological traits of bivalve were induced by metal toxic effects, relating to metal bioaccumulation, subcellular partitioning, and biological susceptibility. There are variations in susceptibility estimations due in part to the site-specific water qualities and the interspecific differences. In this study, a critical parameters such as uptake (k_u), elimination (k_e), killing (k_k), and damage recovery (k_r) rate constants play the key roles in determining the susceptibility estimation to green mussel *P. viridis* and marine clam *R. philippinarum* exposed to waterborne Zn. The susceptibility risks of *R. philippinarum* in Toucheng, Kouhu, and Pingtung of Taiwan region were more significant than that of *P. viridis* (Fig. 6). Both of these aquatic species have similar positive accumulated Zn capacities. However, *P. viridis* has a highest uptake ability than that of *R. philippinarum* (Chong and Wang, 2001). The Zn uptake rate constants to *R. philippinarum* ranged from 65 – 234 mL g⁻¹ d⁻¹, that were much less than uptake rate constant of *R. philippinarum* (637 mL g⁻¹ d⁻¹) (Chong and Wang, 2001; Shi and Wang, 2004). The elimination rate constant of Zn estimated in previous studies with a comparison between *P. viridis* and *R. philippinarum*, revealed that *P. viridis* had a high elimination rate ranging from 0.029 to 0.076 d⁻¹, whereas *R. philippinarum* ranged from 0.023 to 0.026 d⁻¹ (Chong and Wang, 2001; Blackmore and Wang, 2002;

Shi and Wang, 2004). Tang et al. (2009) indicated that metal elimination capacity was decisive for depiction of exposure pathway in *P. viridis*.

Previous studies indicated that *P. viridis* triggered the regulatory mechanism to maintain physiological metal content nearly $100 \mu\text{g g}^{-1}$ accumulation levels in tissue when exposed to $100 - 300 \mu\text{g L}^{-1}$ waterborne Zn (Chan, 1988; Tang et al., 2009). This present study seems reasonable to conclude that green mussel is positive bioregulation since the slightly killing level ($0.025 \text{ g mg}^{-1} \text{ d}^{-1}$) and high elimination ability were better than marine clam. Our present study adopted a great deal of Zn toxicokinetics of bivalve in Hong Kong area to reanalyze the bioconcentration factor probability that were approximately 12000 mL g^{-1} (Chong and Wang, 2001; Blackmore and Wang, 2002; Shi and Wang, 2004). Tang et al. (2009) have been measured waterborne and bivalve tissue of Zn concentration in southern Taiwan area, by which the bioconcentration factor can be calculated to be $5304 - 8871 \text{ mL g}^{-1}$. If the Zn bioconcentration factor in southern Taiwan area is feasible to bivalve that the susceptibility risk assessment may exist overvalue. Nevertheless, our results show that Zn posed no significant susceptibility risk to two bivalve species in Taiwan.

4.3 Implications

One of the major challenges in aquatic risk assessment is improving our predictive power of adverse effects caused by realistic exposure conditions. Traditionally, ambient water quality criteria (AWQC) or permit limits were derived from a series of toxicity bioassays based on the total external concentration concept. To characterize the dose-response relationship more precisely, some approaches including water effect ratio, biotic ligand model, free ion activity model, and biokinetic model have been developed and used in the last decade to delineate the bioavailability and bioaccumulation mechanisms involved in the metal transport

processes from external concentration in water to whole body burden in organisms (De Schamphelaere and Janssen, 2002; Morgan and Wood, 2004; Bielmyer et al., 2007; Luoma and Rainbow, 2008; Chen et al., 2009). Based on the receptor theory in toxicology, some studies have switched the whole body burden to target organ concentration by physiologically-based pharmacokinetic model to further clarify the dose-response relationship (Ling et al., 2005; Clewell et al., 2008). Nowadays, new techniques make it possible to directly relate the physiological toxic effects to the subcellular partitioning of xenobiotics in organisms. Subcellular partitioning model is suggested by some recent studies to predict metal toxicity more accurately since it considers the internal distribution of metals inside the organisms (Wang and Rainbow, 2006; Pan and Wang, 2008). In this study, we developed a mechanistic model, by coupling the bioaccumulation and coping mechanisms, to predict site-specific susceptibility probability of bivalves exposed to waterborne Zn in selected coastal areas in Taiwan. Consequently, we believe that the methodology established here can be employed to better assess the hazardous effects of aquatic organisms associated with metal exposure and, moreover, to refine the existing water quality criteria for the protection of aquatic species.

The subcellular partitioning concept has also been employed by a number of studies to demonstrate the transport of metals along food chain in aquatic ecosystems (Wallace and Luoma, 2003; Cheung and Wang, 2005; Luoma and Rainbow, 2008). Generally, the partitioning of metals to organelles and the two soluble fractions including heat-sensitive proteins and metallothionein-like proteins are considered trophically available to predators. Thus the assimilation efficiency in predators is positively correlated with the trophically available fractions of metals in preys. Recently, He et al. (2010) extended this concept to study the correlation between

bioaccessibility and subcellular fractionation of metals in marine fish, and suggested that the subcellular distribution should be considered to better assess human health risk associated with seafood consumption. In the present study, the correlations among elimination, detoxification, and recovery abilities of bivalves under Zn stress were well established, which enables us to calculate the values of k_r and % detoxified in MDP by the experiment-determined biokinetic parameter, k_e . Therefore, the framework conducted here could provide valuable information and useful tools not only in the trophic transfer of metals along aquatic food chain, but also in the subsequent human health risk assessments.

5. Conclusion

In the present study, a comprehensive modeling framework was developed to predict susceptibility probability of two bivalve species exposed to waterborne Zn. Estimation of the biokinetic and toxicokinetic parameters in derived models indicated that *P. viridis* accumulates more Zn toxicity, whereas both toxic potency and the speed of recovery of Zn are higher for *R. philippinarum*. Simulation results showed that the spatial differences of susceptibility primarily resulted from the variation of waterborne Zn concentration under field conditions. Furthermore, *R. philippinarum* is more susceptible of Zn than *P. viridis* under the same exposure condition. Results also suggested that Zn posed no significant susceptibility risk to two bivalve species in Taiwan. Finally, the results of this study implied that in order to enhance our ability in ecological and human health risk assessment, it is important to consider the trophic transfer of metals based on the subcellular partitioning concepts.

References

- Ashauer, R., Boxall, A.B.A., Brown, C.D., 2007. New ecotoxicological model to simulate survival of aquatic invertebrates after exposure to fluctuating and sequential pulses of pesticides. *Environ. Sci. Technol.* 41, 1480–1486.
- Bielmyer, G.K., Grosell, M., Paquin, P.R., Mathews, R., Wu, K.B., Santore, R.C., Brix, K.V., 2007. Validation study of the acute biotic ligand model for silver. *Environ. Toxicol. Chem.* 26, 2241–2246.
- Blackmore, G., Wang, W.X., 2002. Uptake and efflux of Cd and Zn by green mussel *Perna viridis* after metal preexposure. *Environ. Sci. Technol.* 36, 989–995.
- Chan, H.M., 1988. Accumulation and tolerance to cadmium, copper, lead and zinc by green mussel *Perna viridis*. *Mar. Ecol. Progr. Ser.* 48, 295–303.
- Chen, B.C., Chen, W.Y., Liao, C.M., 2009. A biotic ligand model-based toxicodynamic approach to predict arsenic toxicity to tilapia gills in cultural ponds. *Ecotoxicology* 18, 377–383.
- Cheung, M., Wang, W.X., 2005. Influence of subcellular metal compartmentalization in different prey on the transfer of metals to a predatory gastropod. *Mar. Ecol. Progr. Ser.* 286, 155–166.
- Chong, K., Wang, W.X., 2001. Comparative studies on the biokinetics of Cd, Cr, and Zn in the green mussel *Perna viridis* and the Manila clam *Ruditapes philippinarum*. *Environ. Pollut.* 115, 107–121.
- Clewell, H.J., Tan, Y.M., Campbell, J.L., Andersen, M.E., 2008. Quantitative interpretation of human biomonitoring data. *Toxicol. Appl. Pharmacol.* 231, 122–133.
- Croteau, M., Luoma, S.N., 2009. Predicting dietborne metal toxicity from metal

- influxes. *Environ. Sci. Technol.* 43, 4915–4921.
- De Schamphelaere, K.A., Janssen, C.R., 2002. A biotic ligand model predicting acute copper toxicity for *Daphnia magna*: the effect of calcium, magnesium, sodium, potassium, and pH. *Environ. Sci. Technol.* 36, 48–54.
- He, M., Ke, C.H., Wang, W.X., 2010. Effects of cooking and subcellular distribution on the bioaccessibility of trace elements in two marine fish species. *J. Agric. Food Chem.* 58, 3517–3523.
- Kamunde, C., 2009. Early subcellular partitioning of cadmium in gill and liver of rainbow trout (*Oncorhynchus mykiss*) following low-to-near-lethal waterborne cadmium exposure. *Aquat. Toxicol.* 91, 291–301.
- Lee, C.L., Chen, H.Y., Chuang, M.Y., 1996. Use of oyster, *Crassostrea gigas*, and ambient water to assess metal pollution status of the charting coastal area, Taiwan, after the 1986 green oyster incident. *Chemosphere* 33, 2505–2532.
- Lee, J.H., Landrum, P.F., Koh, C.H., 2002. Prediction of time-dependent PAH toxicity in *Hyalella azteca* using a damage assessment model. *Environ. Sci. Technol.* 36, 3131–3138.
- Liao, C.M., Chen, B.C., Singh, S., Lin, M.C., Liu, C.W., Han, B.C., 2003. Acute toxicity and bioaccumulation of arsenic in tilapia (*Oreochromis mossambicus*) from a blackfoot disease area in Taiwan. *Environ. Toxicol.* 18, 252–259.
- Liao, C.M., Jau, S.F., Lin, C.M., Jou, L.J., Liu, C.W., Liao, V.H.C., Chang, F.J., 2009. Valve movement response of freshwater clam *Corbicula fluminea* following exposure to waterborne arsenic. *Exotoxicology* 18, 567–576.
- Liao, C.M., Jou, L.J., Chen, B.C., 2005. Risk-based approach to appraise valve closure in the clam *Corbicula fluminea* in response to waterborne metals. *Environ. Pollut.* 135, 41–52.

- Liao, C.M., Lin, C.M., Jou, L.J., Chen, W.Y., 2008. Sodium gill potential as a tool to monitor valve closure behavior in freshwater clam *Corbicula fluminea* in response to copper. *Sensors* 8, 5250–5269.
- Ling, M.P., Liao, C.M., Tsai, J.W., Chen, B.C., 2005. A PBTK/TD modeling-based approach can assess arsenic bioaccumulation in farmed tilapia (*Oreochromis mossambicus*) and human health risks. *Integr. Environ. Assess. Manag.* 1, 40–54.
- Luoma, S.N., Rainbow, P.S., 2008. *Metal Contamination in Aquatic Environments*. Cambridge University Press, New York.
- Martin, C.A., Luoma, S.N., Cain, D.J., Buchwalter, D.B., 2007. Cadmium ecophysiology in seven stonefly (Plecoptera) species: delineating sources and estimating susceptibility. *Environ. Sci. Technol.* 41, 7171–7177.
- Morgan, T.P., Wood, C.M., 2004. A relationship between gill silver accumulation and acute silver toxicity in the freshwater rainbow trout: support for the acute silver biotic ligand model. *Environ. Toxicol. Chem.* 23, 1261–1267.
- Ng, T.Y.T., Wang, W.X., 2004. Detoxification and effects of Ag, Cd, and Zn pre-exposure on metal uptake kinetics in the clam *Ruditapes philippinarum*. *Mar. Ecol. Prog. Ser.* 268, 161–172.
- Pan, K., Wang, W.X., 2008. The subcellular fate of cadmium and zinc in the scallop *Chlamys nobilis* during waterborne and dietary metal exposure. *Aquat. Toxicol.* 90, 253–260.
- Sappal, R., Burka, J., Dawson, S., Kamunde, C., 2009. Bioaccumulation and subcellular partitioning of zinc in rainbow trout (*Oncorhynchus mykiss*): cross-talk between waterborne and dietary uptake. *Aquat. Toxicol.* 91, 281–90.
- Shi, D., Wang, W.X., 2004. Understanding the differences in Cd and Zn bioaccumulation and subcellular storage among different populations of marine

- clams. *Environ. Sci. Technol.* 38, 449–456.
- Tang, C.H., Lin, C.S., Wang, W.H., 2009. Metal accumulation in marine bivalves under various tributyltin burdens. *Environ. Toxicol. Chem.* 28, 2333–2340.
- Tsai, J.W., Liao, C.M., Liao, V.H.C., 2006. A biologically based damage assessment model to enhance aquacultural water quality management. *Aquaculture* 251, 280–294.
- Wallace, W.G., Luoma, S.N., 2003. Subcellular compartmentalization of Cd and Zn in two bivalves. II. Significance of trophically available metal (TAM). *Mar. Ecol. Prog. Ser.* 257, 125–137.
- Wang, W.X., Rainbow, P.S., 2006. Subcellular partitioning and the prediction of cadmium toxicity to aquatic organisms. *Environ. Chem.* 3, 395–399.

Figure caption

Fig. 1. Schematic representation of computational algorithm to predict the susceptibility of bivalve exposed to waterborne zinc and the site-specific susceptibility risk assessment. $LN(a, b)$ represents lognormal distribution with geometric mean a and geometric standard deviation b .

Fig. 2 (A, B) Probability distribution of bioconcentration factor (BCF) for *P. viridis* and *R. philippinarum* exposed to waterborne zinc. (C, D) Optimal fits of %zinc in MT applied by DAM-based safety function for *P. viridis* and *R. philippinarum* exposed to waterborne zinc.

Fig. 3 (A) Lognormal probability distribution of elimination rate constant (k_e) varied with waterborne zinc $0 - 250 \mu\text{g L}^{-1}$ for *P. viridis* and (D) *R. philippinarum*. (B) Lognormal probability distribution of detoxification rate constant (k_d) varied with waterborne zinc $0 - 250 \mu\text{g L}^{-1}$ for *P. viridis* and (E) *R. philippinarum*. (C) The joint distribution showing the quantitative relationship between k_e and k_d varied with waterborne zinc $0 - 250 \mu\text{g L}^{-1}$ for *P. viridis* and (F) *R. philippinarum*.

Fig. 4 (A, G; B, H; C, I) Relationship between k_e and k_d , k_d and k_r , k_e and k_r in *P. viridis* and *R. philippinarum* exposed to $50 \mu\text{g L}^{-1}$ waterborne zinc, respectively. (D, J; E, K; F, L) Probability distribution of k_d , k_d and k_r in *P. viridis* and *R. philippinarum*, respectively.

Fig. 5 Site-specific probability distribution of waterborne zinc concentration for cultural farms located at (A) Toucheng, (C) Kouhu, and (E) Anping in Taiwan. (B, D, F) Predicted site-specific susceptibility risk assessments in *P. viridis* and *R. philippinarum* cultural farms of Toucheng, Kouhu, and Anping, respectively.

Table 1

Input parameters and parameter estimations for the damage assessment model (DAM) fitted to % zinc in MT of *P. viridis* and *R. philippinarum*

	<i>P. viridis</i>	<i>R. philippinarum</i>
Input parameter		
k_u (mL g ⁻¹ d ⁻¹)	637 ^a	234 ^a
k_e (d ⁻¹)	0.050	0.019
$C_{MAP,C}$ (μg g ⁻¹)	71.33	36
Parameter estimates		
k_k (g mg ⁻¹ d ⁻¹)	0.025	0.13
k_r (d ⁻¹)	0.19	0.40

^a Adopted from Chang and Wang (2001).

Fig. 1.

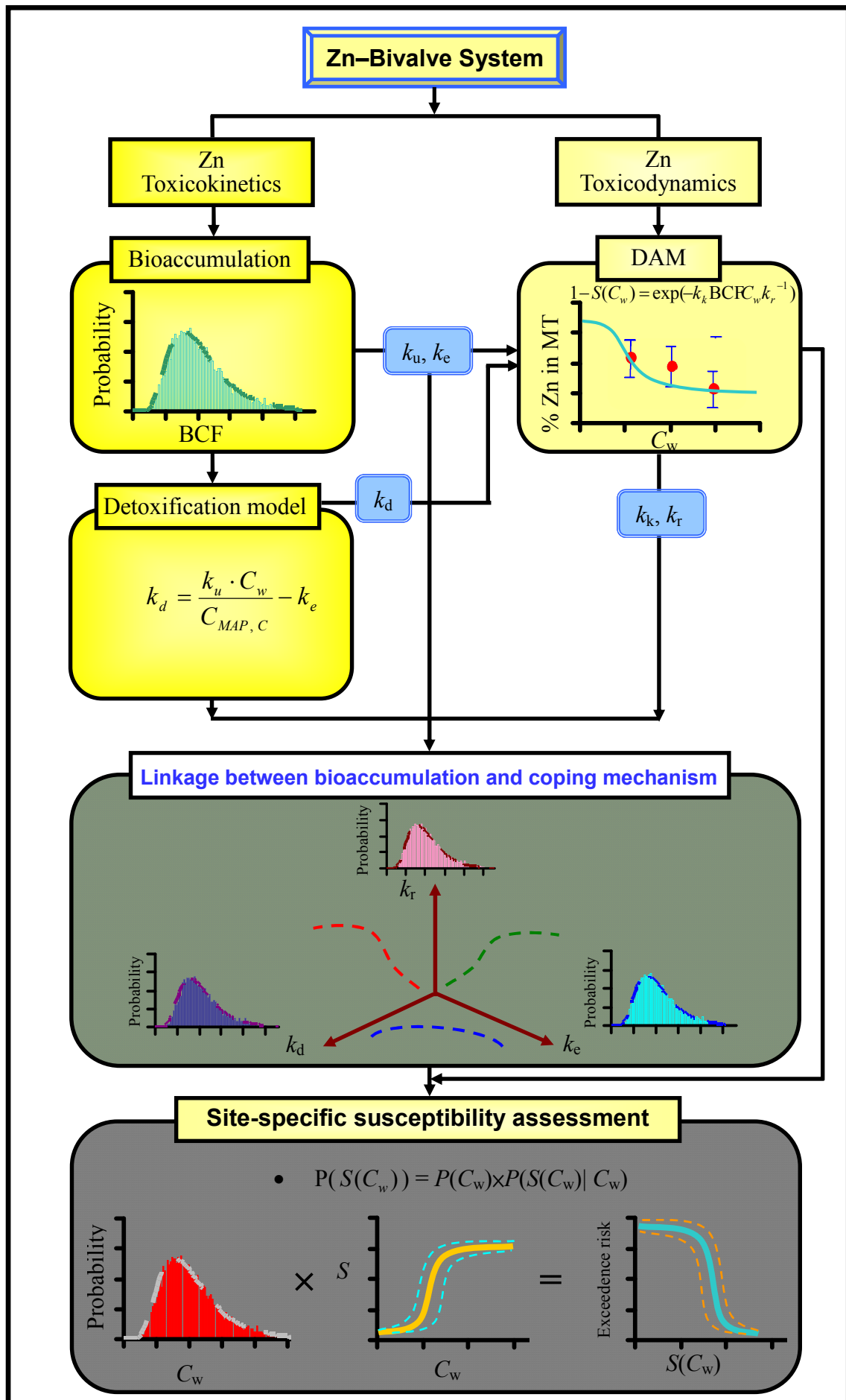


Fig. 2.

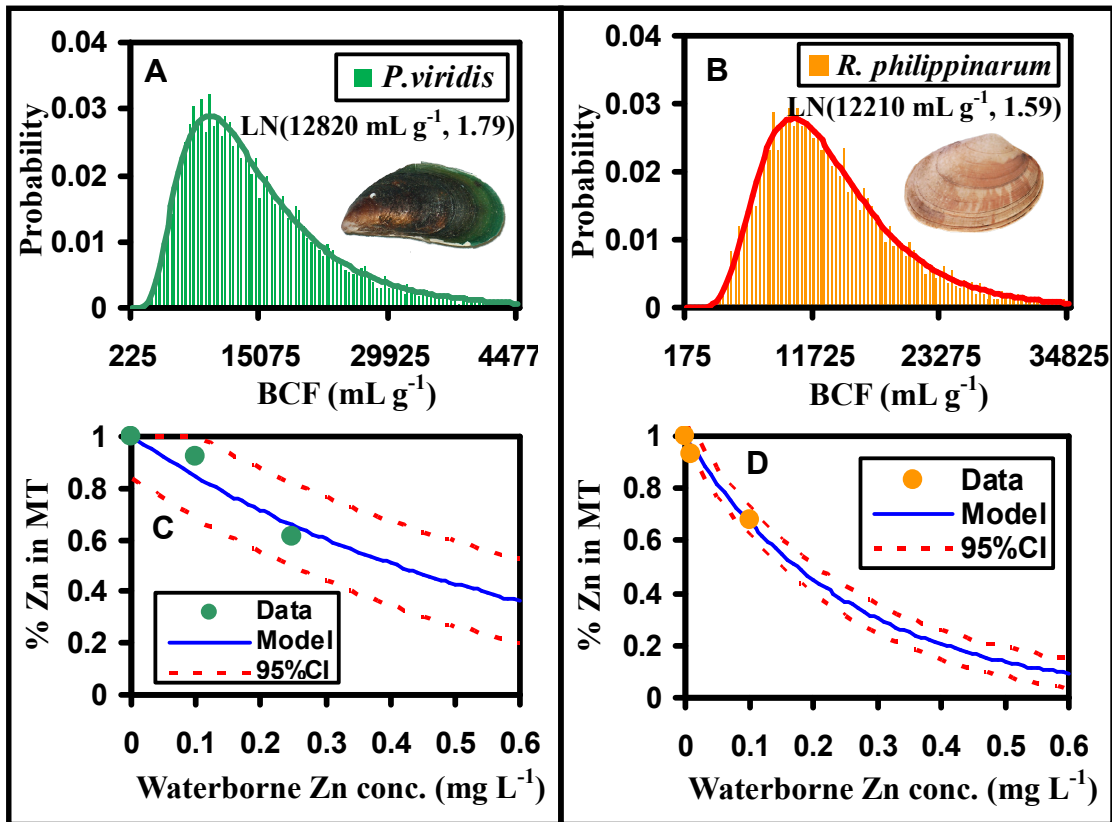


Fig. 3.

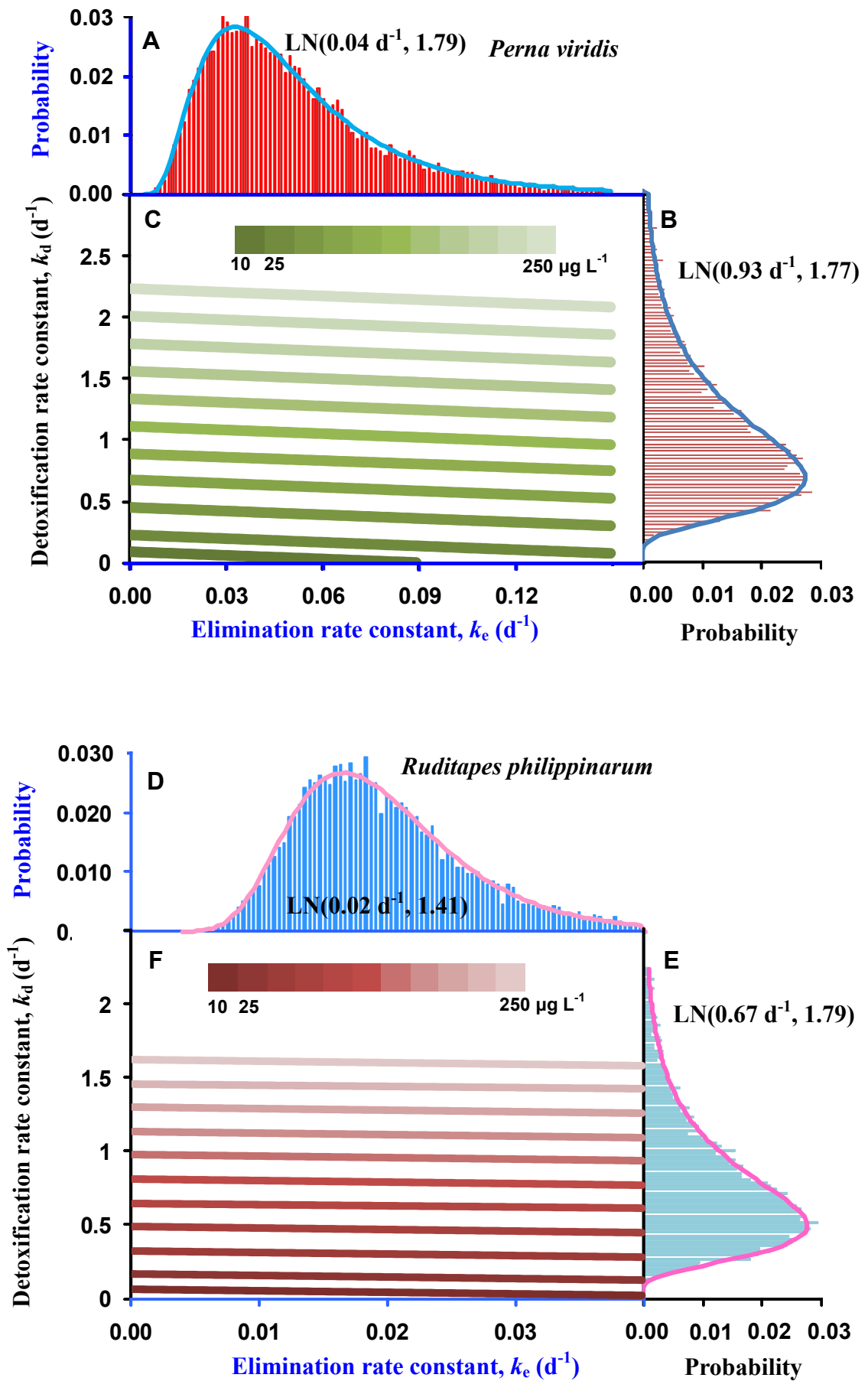


Fig. 4.

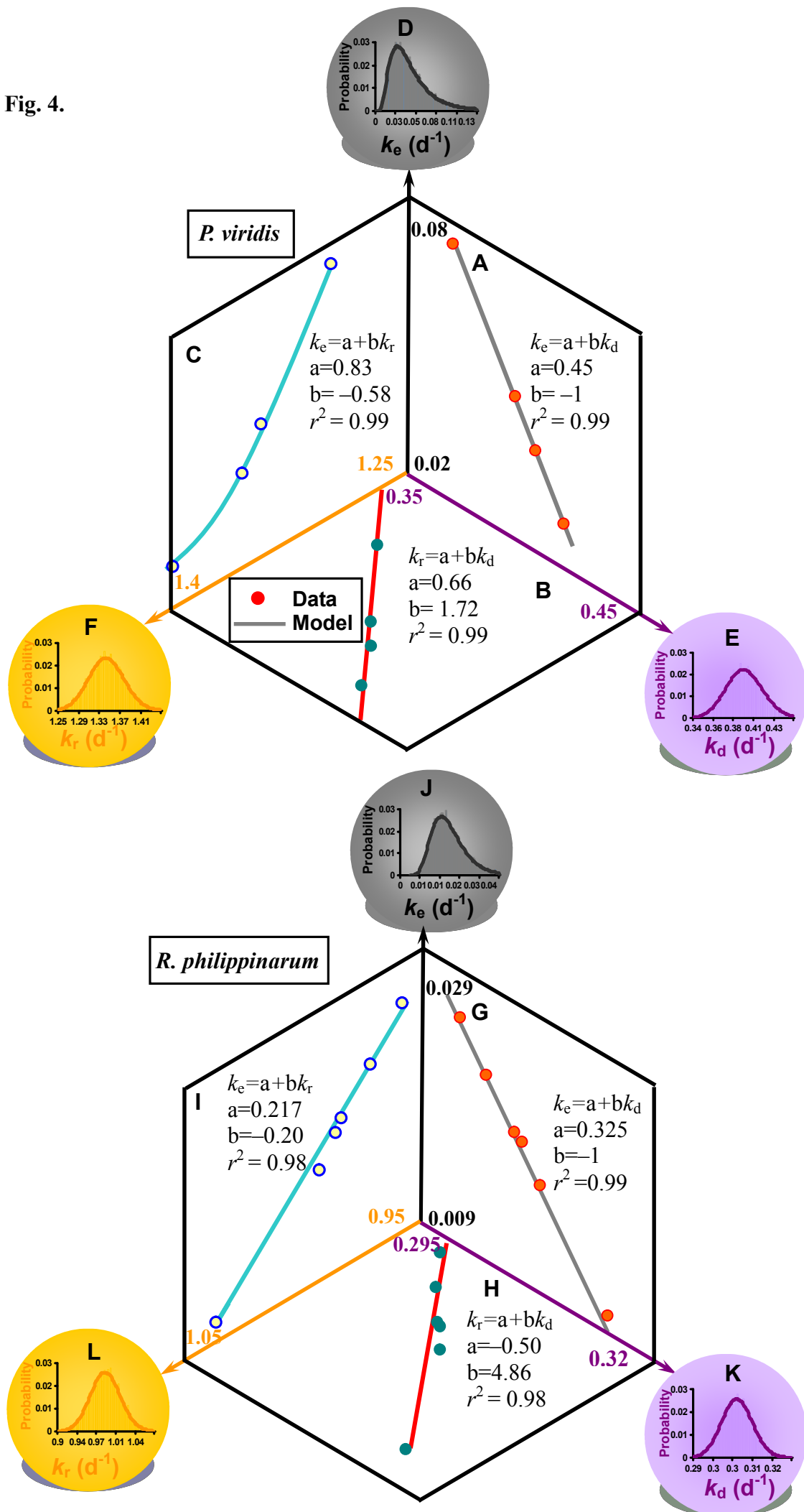


Fig. 5.

